AUTHOR(S): GUPTA, R., PANCHOLI, K., PRABHU, R., PANCHOLI, M., HUO, D., JHA, V. and LATTO, J.

TITLE: Integrated self-healing of the composite offshore structures.

YEAR: 2017

Publisher citation: GUPTA, R., PANCHOLI, K., PRABHU, R., PANCHOLI, M., HUO, D., JHA, V. and LATTO, J. 2017. Integrated self-healing of the composite offshore structures. In Proceedings of the 60th MTS/IEEE OCEANS conference (OCEANS'17): a vision for sustaining our marine futures, 19-22 June 2017, Aberdeen, UK. New York: IEEE [online], article ID 8084828. Available from: https://doi.org/10.1109/OCEANSE.2017.8084828

OpenAIR citation: GUPTA, R., PANCHOLI, K., PRABHU, R., PANCHOLI, M., HUO, D., JHA, V. and LATTO, J. 2017. Integrated self-healing of the composite offshore structures. In Proceedings of the 60th MTS/IEEE OCEANS conference (OCEANS'17): a vision for sustaining our marine futures, 19-22 June 2017, Aberdeen, UK. New York: IEEE, article ID 8084828. Available from: https://openair.rgu.ac.uk

Integrated self-healing of the composite offshore structures

Ranjeetkumar Gupta, Ketan Pancholi*, Radhkrishna Prabhu.
School of Engineering,
Robert Gordon University,
Aberdeen, UK
*k.pancholi2@rgu.ac.uk

Mehul Pancholi
Technology and Innovation
Linde Group,
Guildford, UK

Vineet Jha, James Latto
Composite Department,
GE Oil and Gas,
Newcastle-u-Tyne, UK

Dehong Huo
School of Mechanical and System Engineering,
Newcastle University,
Newcastle upon Tyne, UK

***Abstract*— The self-repairing composite materials integrated with sensing is way forward to reduce maintenance cost and increase consumer safety. In this work, the novel self-healing carbon fibre reinforced unidirectional bulk tape of simple architecture is prepared using nanocomposite film. The bulk material tape was prepared using nanocomposite film of low melting temperature polymer sandwiched between two carbon fibre reinforced unidirectional tapes. First, the nanocomposite polyamide 6 (PA 6) tape with iron oxide nanoparticle was prepared using in-situ polymerization and mixing method. The iron oxide nanoparticle was silane coated suing tri-phasic reverse emulsion method to achieve better dispersion in PA 6 matrix. The nanocomposite was characterized using FTIR, XRD, DSC and TEM. Result shows that the proposed method of preparing self-healing bulk tape material has potential to be used for self-healing composite structure.**

Keywords—component; self-healing; intelligent material; nanocomposite, composite, iron oxide, nanoparticles, in-situ polymerization

I. INTRODUCTION

Conventional approaches of managing damage detection of protective coatings or composite material and subsequent manual repair/replacement involves costly and time consuming preventive maintenance [1]. While approaches to improve polymer matrix composite's (PMC) tolerance to mechanical stresses either by optimising or developing new polymer matrices and structural reinforcements have proven fruitful, however, existing technologies remain suboptimal for future needs. Preventing failure via simultaneous detection and repair rather than using stronger material represents a novel, more flexible solution towards improving materials performance. Self-healing gives best performance for first 5-6 times and the rate of crack extension was reduced by 80% (experimentally) [2].

Many different systems have been proposed for self-healing material system, mainly, an extrinsic vascular system and intrinsic nanoparticle incorporated nanocomposite healing system. Vascular networks can easily be introduced into carbon fibre layers, however, vascular network filled with liquid can influence overall strength of the material, especially when vascular network is dense. Dense vascular networks can also aid in preventing common failure modes within CFRP such as delamination. This, however, would still have a limited number of healing cycles, since the vascular network would become blocked over time.

With a nanoparticle self-healing polymer, repetitive healing would not be an issue as thermoplastics with dispersed iron oxide can be melted to fill cracks multiple times, allowing multiple healing cycles to be undertaken. To ensure the maximum healing potential was created within CFRP samples, long strands of polymer with iron oxide nanoparticles dispersed within them could be directly embedded into CFRP

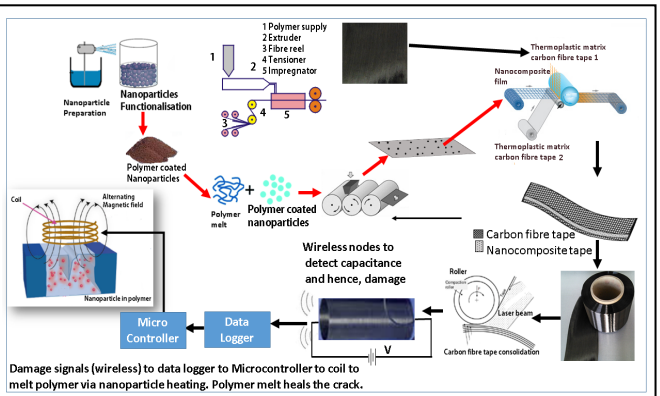

Figure 1: Schematic showing concept of bulk sandwich tapes with processing steps to prepare tubular structure and its intelligent healing process using magnetic flux stimuli.

layers. This would create a similar network as in the vascular system, providing the increased strength but allowing for multiple healing cycles to take place, hence creating a hybrid

healing system. Preparing nanocomposite is complex task which requires homogenous or hierarchical dispersion of nanoparticles. Intelligent repairing in this component worked in two steps:

1. Carbon fibres present in the composite was connected to a power source enabling measurement of capacitance across the component to detect any crack/void/delamination.
2. The damage detection triggers magnetic flux and melts the polymer matrix that fills the crack and voids.

In this work, firstly, the PA6 material with iron oxide nanoparticle was prepared. Resulting nanocomposite film was a sandwiched between unidirectional carbon fibre reinforced thermoplastic (PA 12) tape. The stimuli, heated the nanoparticles to melt the polymer surrounding them and filled the crack/voids to repair the defect when the thermoplastic solidifies.

II. Materials and Methods

A. Materials

Iron (III) oxide nanoparticles (NPs) with <50 nm particle size (BET), ε-caprolactam (CL) (99% purity), Ethylmagnesium bromide (EtMgBr) solution 3.0 M in diethyl ether, N-acetyl caprolactam (NACL) (99% purity), (3-Aminopropyl) triethoxysilane (APTES) (99% purity) and Span-85 were purchased from Sigma-Aldrich Company Ltd. Dorset, UK. Other laboratory agents were used as standard.

B. Experimental

Firstly, 150 mg of iron oxide particles were introduced into a mixture of 30ml toluene and 5g of span-85 [3]. The mixture was shaken to form a tri-phasic reverse emulsion (TPRE). APTES was added to a final concentration of 2% w/v and the

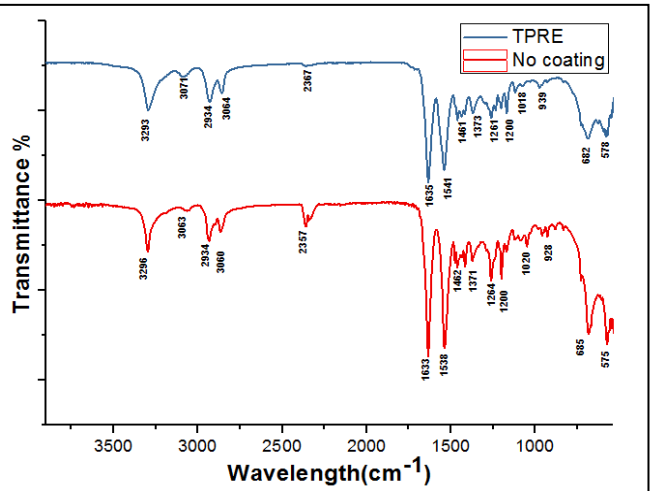

Figure 2. ATR-FTIR Spectra of polymer nanocomposite samples.

mixture was allowed to react in condenser at 50 °C in an oil bath for 5 hrs with constant stirring. The nanoparticles were separated using decantation and washed with coupling solution of 0.8% (v/v) glacial acetic acid in dry methanol, three times and was stored in the same solution at room temperature.

For synthesising the polymer nanocomposite, the silane coated NPs were washed with de-ionized water prior to use. Now, 15g of CL was taken in a two-necked round bottom flask and melted at 90 °C, then the NPs were introduced and the mixture was subjected to sonication at 20 KHz for 20 minutes, to ensure uniform dispersion. Further the mixture was brought to 155 °C, and 0.43ml of EtMgBr followed by 0.47ml of NACL were introduced from one neck while maintaining continual nitrogen supply throughout the process from the other. Because EtMgBr is efficient anionic initiator, the polymerisation of CL was very quick and has taken place in less than minute. Therefore, the nanoparticles did not settled down at the bottom of the flask and most were captured in polymer.

C. Characterisation

To observe the effect of nanoparticle addition on chemical bonds during polymerisation of nanocomosite, the Perking Elmer Attenuated Total Reflection- Fourier Transmission Infrared (ATR-FTIR) Spectrum Gx system with DGS-KBr sensor at a resolution of 4 $cm^{-1}$was used. A 100 µm nanocomposite film was prepared and scanned 30 times to obtain transmission spectrum in range of a wavelength 525-4000 cm^{-1}. The set gain was of two and optical velocity set to 0.4747 (m/s).

Differential scanning calorimetry (DSC) was carried to

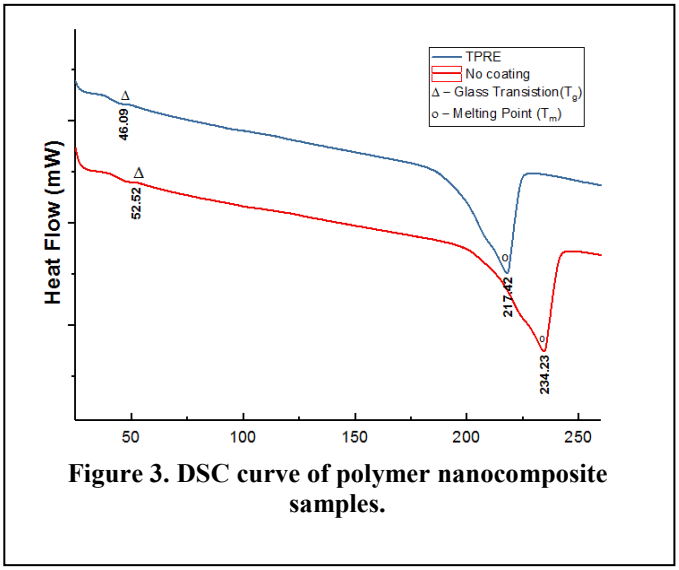

Figure 3. DSC curve of polymer nanocomposite samples.

determine effect of nanoparticle addition on transformation temperature of pure polymer PA 6, by observing the shift in the glass transition temperature (T_g) and melting temperature (T_m). The TA Instruments DSC Q100 was used to characterise 9 mg of nanocomposite placed in alumina crucible at a heating rate of 10°C/min under a nitrogen environment with a temperature range of 20 to 270°C. The care was taken to remove any residue in alumina crucible by sintering in oven at 500 °C.

Authors thanks RGU for providing funding for this work

Furthermore, the NPs with and without silane coating were characterised using Transmission Electron Microscopy (TEM). The nanoparticles were dispersed in very small amount of solvent and sonicated before placing 10 ml of solvent on Gilder copper TEM grid of 400 mesh. The dispersion and agglomeration condition in polymer was determined using X-ray diffraction (XRD) using diffractometer using CuKα radiation in the 2θ range from 10 to 65. The TEM was carried out at an operating voltage of 100 kV with the spot size 10nm. Various magnifications were used ranging from x7900 to x245000 on the Philips CM100 TEM to capture the micrographs of nanoparticles.

III. Results and Discussion

The observance of the various peaks as shown in Figure 2, matches with the commercial samples standard template in the FTIR, which hints efficacious creation of PA6. The amine peak at 3293 cm^{-1} attributed to N-H bond and the one at 2934 cm^{-1} corresponding to methylene stretch vibrations of asymmetric and symmetric nature, reflect as those typically found in PA6 [4].

The presence of the amide II band of primary amides, occurring due to stretching vibration of the C=O double bond,

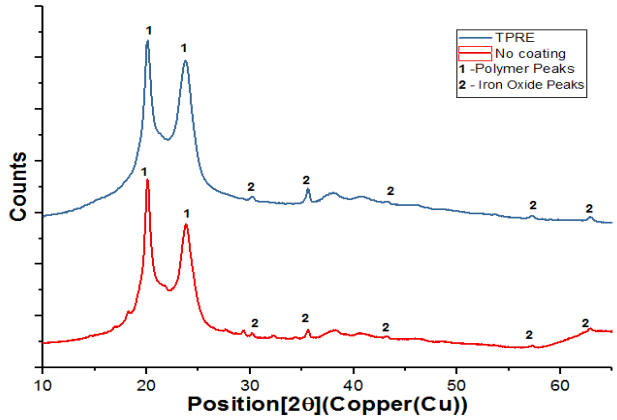

Figure 4. XRD patterns of polymer nanocomposite samples.

and further attributing to the functionality of the amide I band is observed from 1541 cm^{-1} - 1635 cm^{-1}, also an additional peak at 1540 cm^{-1} due to amide I and II bands of the primary type, but also pointing vibration due to stretching of the C-N bond, which then results in a vibration due to bending of the N-H bond, and the CONH bond [5]. The degree of crystallinity is generally dictated by the position and intensity of these crystalline bands, as well as the broader bands from the amorphous phase [6]. Thus it can be seen that the degree of crystallinity is moderately high in most of the polymer samples, as the amide II band, which is considerably sensitive to the crystalline structure, appears around 1540 cm^{-1}. Furthermore, the peak around 3080 cm^{-1} is due to the amide B band of the polymer [7] The sharp peaks occurring at 580 cm^{-1} and 690 cm^{-1} are seen to be a result of the out-of-plane bends of the N-H bond, native to band V of the amide group, and the C=O double bond, native to band VI of the amide group [5]. The sharp peaks around 1460 cm^{-1} and 1370 cm^{-1} correspond to the vibration caused by the CH_2 groups joining the CO and NH bonds, with the doublet seen at 1465 and 1440 cm^{-1} corresponding to the amorphous and γ-phases[8].

The DSC results as presented in Figure 3, depicts a noticeable endothermic peak referring to the glass transition of the polymer samples, occurring at 46.09 °C for TPRE sample. This is clearly shifted from the 52.52 °C for the no coating sample. And the melting temperature of the TPRE sample is sufficiently lowered to 217.42 °C, which proves a susceptible application of this sample for self-healing applications. The heat fusion as taken from the thermogram was analysed to calculate percentage crystallinity; and was found to be 72.76% and 58.89% for uncoated and coated using TPRE method, respectively.

In the XRD pattern(Figure 4) the two-dominant monoclinic crystallite phases viz. the α-phase indexed as (200) and

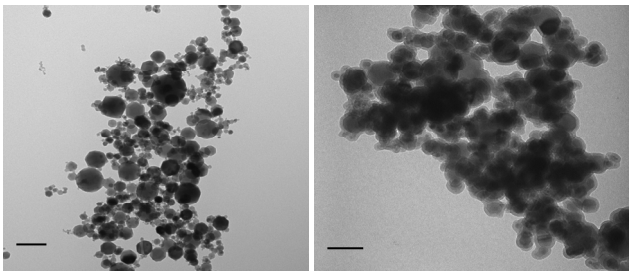

Figure 5. TEM micrographs of NPs, from left to right: Uncoated NPs and TPRE NPs (scale bar 100

(002)/(202), and γ-phase with corresponding indexes of (020), (001) and (200)/(201), are seen to appear at around 21° and 24°; confirming the prominent PA-6 presence in the sample[5]. The crystallite sizes of NPs were calculated from FWHM of

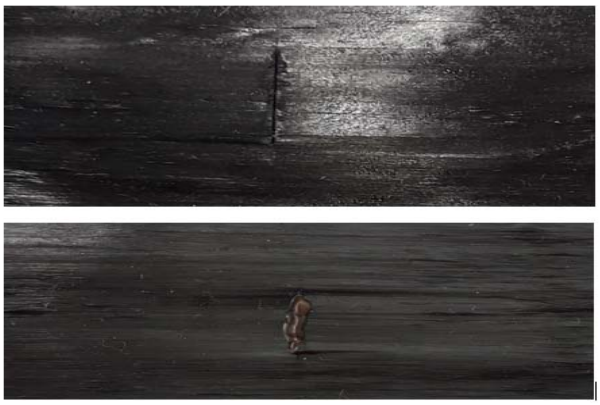

Figure 6. Damaged sample and repair after heating of the sample (top to bottom).

the most intense peaks using the Debye–Scherrer formula; giving an approximate crystallite size of 41.76 nm and 30.93 nm for uncoated and coated particles with TPRE method, respectively. This infers that the particle dispersion has improved due to decrease in crystallite size. As seen in Figure

4, a mixture of crystalline and amorphous phases were seen, showing poly-ordered polycrystalline phases responsible for amorphous phase; and assuring that the polymer itself is a mixture of amorphous and crystalline phase.

TEM images were taken to finally confirm the effect on the particle distribution, agglomeration status and validate particle size finding results obtained using XRD. As shown in Figure 4, TEM micrographs show that the NPs have been fully coated in silane using TPRE, Figure 5 shows the effect of coated on particles.

The carbon fibre reinforced tapes were consolidated and added and attached to two electrodes to measure the impedance. The impedance was measured before and after the crack has developed. The tubular structure made of the layered tape was subjected to point load until delamination and transverse crack was occurred. Initial measurements showed that the capacitance across the tubular structure was changed from 697.4 pF to 665.2 pF.

Finally, the synthesized polymer nanocomposite was placed between two carbon fibre reinforced polymer unidirectional tapes. To test its self-healing capability, a cut is made on the sample of mulilayer carbon fibre reinforced tape. A cut was made on the tape made up of polymer nanocomposite film sandwiched between two layers of the tape, and a crack was created on the surface before generating heat, as shown in Figure 6.

In response to the heat, the polymer nanocomposite layer acted as a sacrificial layer and melted to fill the crack. The polymer PA 6 which absorbed heat from the nanoparticles has melted easily within two minutes. Because nanoparticles acted as receptors to stimuli, the melting of PA6 has taken place at quicker rate. This shows the time efficacy of the self-healing ability of the synthesised nanocomposite.

REFERENCES

[1] Anderson et al., Self-healing polymers and composites. Vol. 100 of the series Springer Series in Materials Science pp 19-44 Self-Healing Materials, (2007)

[2] A.R. Hamilton et al, Mitigation of fatigue damage in self-healing vascular materials, Polymer, 53 (24) (2012), 5575–5581

[3] W. Stober, A. Fink, and E. Bohn, "Controlled growth of monodispersed silica spheres in the micron size range." in J. Colloid. Interface. Sci. 26, 1968, pp. 62–69.

[4] D. Tunc, H. Bouchekif, B. Améduri, C. Jérôme, P. Desbois, P. Lecomte and S. Carlotti, "Synthesis of aliphatic polyamide bearing fluorinated groups from ε-caprolactam and modified cyclic lysine." in *European Polymer Journal,* 2015; 71:5. pp. 75-84.

[5] P. S. Kalsi, "Spectroscopy of organic compounds." New Age International; 6th ed., 2007. pp. 107-151.

[6] Y.C. Chen, S.X. Zhou, H.H. Yang and L.M. Wu, "Structure and Properties of Polyurethane/Nanosilica Composites." in Journal of Applied Polymer Science, 95(5), 2005. pp. 1032–1039.

[7] Garidel P, Schott H. Fourier-transform midinfrared spectroscopy for analysis and screening of liquid protein formulations. *BioProcess International*. 2006 Jun;4(6):48-55.

[8] Khodabakhshi K. Anionic polymarisation of caprolactam: an approach to optimising the polymerisation condition to be used in the jetting process. (Doctoral dissertation, © Khosrow Khodabakhshi)

[9] L. Ricco, S. Russo, G. Orefice and F. Riva. "Anionic poly (ε-caprolactam): relationships among conditions of synthesis, chain regularity, reticular order, and polymorphism." in *Macromolecules*. 1999; 32(23):77. pp. 26-31.